Platinum-group element mineralogy and geochemistry of chromitite of the Kluchevskoy ophiolite complex, central Urals (Russia)

F. Zaccarini [a],[*],[1], E. Pushkarev [b], G. Garuti [c]

[a] Department of Applied Geological Sciences and Geophysics, Peter Tunner Str. 5, University of Leoben, A-8700 Leoben, Austria
[b] Russian Academy of Sciences, Ural Branch, Str. Pochtovy per. 7, 620151 Ekaterinburg, Russia
[c] Department of Earth Sciences, Via S. Eufemia 19 University of Modena and Reggio Emilia, I-41100 Modena, Italy

Abstract

We report the results of investigation of chromitites occurring in the Kluchevskoy ophiolite complex of the Russian Urals. The chromite composition suggests crystallization from a boninitic magma in a supra-subduction zone geodynamic setting. The investigated chromitites are enriched in Os–Ir–Ru over Rh–Pt–Pd, as typical of the mantle hosted ophiolite chromitites. Consistent with the geochemical data, the Platinum Group Mineral (PGM) assemblage is dominated by Ru–Os–Ir phases, whilst specific Rh–Pt–Pd minerals are absent. Two distinct paragenetic assemblages have been recognized: 1) primary magmatic PGM (laurite, erlichmanite, osmium, iridium, unnamed Ir–Ni–S, cuproiridsite, irarsite and ruthenarsenite) and 2) secondary PGM formed by desulfurization of primary sulfides at low temperature (ruthenium). Comparison of the studied chromitites with those hosted in the mantle of the Kempirsai, Ray–Iz and Voikar–Sininsky ophiolites has shown that all these chromite deposits form in the same geodynamic environment. The differences in the temperature calculated on the Fe–Mg exchange between olivine–spinel and observed in the PGM assemblage suggest that the Kluchevskoy chromitite suffered the effects of the metasomatism to a lesser extent compared with Kempirsai and Ray–Iz chromitites.
© 2007 Elsevier B.V. All rights reserved.

Keywords: Platinum group minerals; Platinum group elements; Chromitite; Kluchevskoy; Urals; Russia

1. Introduction

In the Ural Mountains, Paleozoic collision between the East European continental platform to the west and the Asian plate to the east brought to the surface a number of mafic–ultramafic complexes. These complexes are main-

ly exposed along the Main Uralian Fault (Fershtater et al., 1997) that extends over more than 2500 km (Fig. 1A), from Kazakhstan to the Ice Sea. The Uralian mafic–ultramafic complexes can be grouped into three main categories: 1) ophiolites in supra-subduction setting, 2) concentrically-zoned complexes emplaced at the root of the island arc (Ural–Alaskan type complexes) and 3) lherzolite–harzburgite mantle and crustal cumulates possibly related with a sub-continental margin (Garuti et al., 1997a; Zaccarini et al., 2004). A major economic feature of the Urals is the widespread occurrence of placer platinum deposits that combine to form one of the largest

---

* Corresponding author. Tel.: +39 059 2055814.
  E-mail address: fedezac@tsc4.com (F. Zaccarini).
[1] Present address: Instituto Andaluz de Ciencias de la Tierra, University of Granada, Campus Fuentenueva s/n, 18002 Granada, Spain.
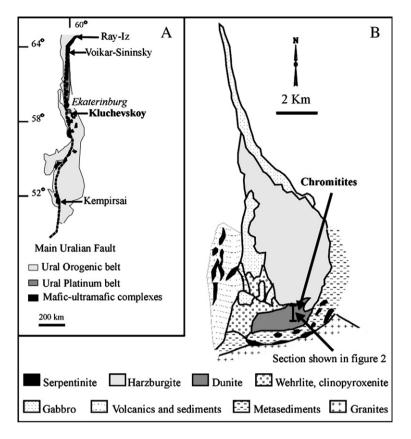
Fig. 1. A = Location of the major ophiolitic complexes and the Platinum belt in the Urals. B = geological map of the Kluchevskoy complex with the location of the geological section shown in Fig. 2.

platinum fields in the world. The platinum in the placers formed by the erosion of platinum-rich dunite and chromitite associated with the Ural–Alaskan type complexes, occurring in the so called Ural Platinum Belt, which is located between 56° and 64° N (Fig. 1A). The Urals are well known among economic geologists for their large deposits of podiform chromitites in the ophiolites of Kempirsai, Kazakhstan, and Ray–Iz and Voikar–Sininsky in the Polar Urals (Fig. 1A). These large chromitite deposits have been extensively investigated for their chromite and platinum group element (PGE) mineralogy and geochemistry (Anikina et al., 1996; Melcher et al., 1997; Economou-Eliopoulos and Zhelyaskova-Panayotova, 1998; Melcher et al., 1999; Garuti et al., 1999a; Kojonen et al., 2003; Distler et al., 2003). Sub-economic chromite deposits occur in many other ophiolite complexes located in the Urals; Kluchevskoy is one of these chromitite occurrences. The Kluchevskoy ophiolite complex is located in the Central Urals, ca. 40 km SE of Ekaterinburg city (Fig. 1A). Contrary to the ophiolite chromitites of Kempirsai, Ray–Iz and Voikar–Sininsky, the Kluchevskoy chromitites have been poorly

investigated for their concentration and mineralogical residence of PGE, and only preliminary results on the occurrence of platinum group minerals (PGM) have been described by Garuti et al. (1999b). In this contribution we report chromite, olivine and PGE mineralogy and geochemistry of the Kluchevskoy chromitites. Our data are also compared with those reported from Kempirsai, Ray–Iz and Voikar–Sininsky, with the aim to verify if, despite their separation, they display some similarities in terms of chromite composition, PGE mineralogy and geochemistry.

2. Geology and sampling

The Kluchevskoy ophiolite complex consists of an allochtonous block covering an area of about 80 km^2 (Fig. 1B). It is composed of harzburgite and dunite of the residual mantle sequence, overlain by a cumulate layered succession of dunite, wehrlite, clinopyroxenite and possibly gabbro, although direct transition between clinopyroxenite and gabbro has never been observed in the field. Several dykes of clinopyroxenite
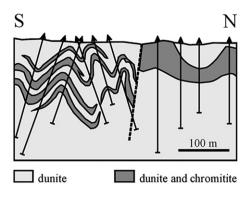
Fig. 2. Geological section of the south-eastern part of the Kluchevskoy complex, showing the location of the chromitites (after Kravchenko, 1986).

have shown that the ore bodies consist of strongly folded, E–W elongated lenses of massive to disseminated chromite, dipping northwards and extending to depths of more than 150 m (Fig. 2) (Kravchenko, 1986).

The geological section of the south-eastern part of the Kluchevskoy complex (Fig. 2) shows that the chromitite bodies are associated with dunite, although it is not possible to recognize if these dunites are located at the Moho transition zone, or within the layered sequence in the complex of Kluchevskoy. Small dunite bodies, containing abundant disseminated chrome spinel, have been also discovered in the central and northern parts of the complex (Kravchenko, 1986). According to past mining exploration, the chromitite bodies of the Kluchevskoy complex yield a total reserve of a few tens of thousands of tons of ore. The Kluchevskoy chromitites have been not exploited so far. The Kluchevskoy complex records several events related to the post-magmatic evolution, possibly involving: 1) oceanic metamorphism; 2) hydrothermal metasomatism produced by the intrusion of a granite body in the southern east part of the complex (Figs. 1B and 3) weathering. The investigated samples were collected from old exploration works, in the southern part of the ophiolite complex. The samples are representative of massive to disseminate chromitites, with about 50 to 70 vol.% of silicate matrix.

and fine-grained gabbro–diorite crosscut both the mantle unit as well as the layered series. A Paleozoic syncollisional granite is exposed in the southern part of the Kluchevskoy complex (Fig. 1B). According to Kravchenko (1986), the maximum thickness of Kluchevskoy complex is ca. 5 km and it is exposed in the southern part of the complex. In this area, dunites with chromitites are the most abundant rocks. Chromitites occur in several localities in the southern part of the complex, in the proximity of the boundary between layered dunite–wehrlite and residual harzburgite of the mantle sequence. Trenching and drilling
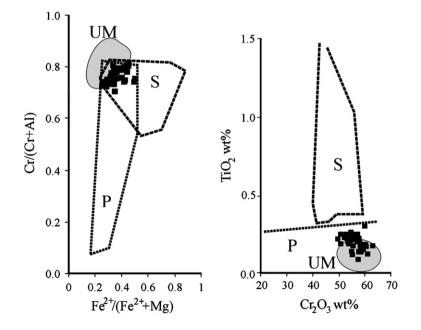

Fig. 3. Chemical composition of chromite from chromitites of Kluchevskoy. Abbreviations: P = podiform chromitites, S = stratiform chromitites, UM = chromitites in the Urals ophiolitic mantle (from Garuti et al., 1999a and unpublished data of the authors). Diagram TiO_2 versus Cr_2O_3 after Ferrario and Garuti (1988).

3. Methodology

Thirty polished sections, obtained from 15 samples of chromitite were investigated by reflected-light microscope. Then, the PGM were studied by electron microscopy and analyzed by electron microprobe. The SEM images were obtained with a Philips Xl-30 scanning electron microscope equipped with an X-ray energy dispersion system (X-EDS) detector (Edax 9900), using an accelerating voltage of 20 to 30 kV and 2 to 10 nA beam current. Quantitative analyses were carried out using an ARL-SEMQ electron microprobe, operated in the wave dispersion system (WDS) mode, at 15 to 25 kV accelerating voltage, and 15 to 20 nA beam current. Compositions of chromite and olivine were obtained from analysis of several grains in each section. Natural silicate and oxide standards were used except for Ni, V, and Zn, for which pure metal standards were used. The proportion of divalent and trivalent iron in chromite plotted in the diagrams was calculated assuming stoichiometry and charge balance. Analyses of chromite and olivine are presented in Tables 1 and 2, respectively. The PGM were analyzed using pure metals as the reference material for PGE, natural pyrite, chalcopyrite and niccolite for Fe, Ni, Cu, S and As. On-line reduction of data and correction of the interferences Ru–Rh, Ir–Cu and Ru–Pd were performed with the Probe software (Donovan and Rivers, 1990). Because of the small size of the grains, variable amounts of Cr and Fe detected in the analyses of PGM included in chromite are ascribed to fluorescence from direct or secondary excitation of the spinel host. Therefore, the analytical results have been recalculated subtracting all the Cr and a proportional amount of Fe, as deduced from the Cr:Fe ratio of the adjacent chromite. Analyses of the PGM, with corrected amounts of Fe, are listed in Table 3.

Two samples of massive chromite and eight samples of mafic–ultramafic rocks were analyzed for PGE and Au by ICP-MS, after the Ni-sulfide preconcentration with Te-coprecipitation. The results are reported in Table 4. Massive chromitite were analyzed at the Geological Survey of Finland. The other rocks were

Table 2
Selected analyses (wt.%) of olivine from different rocks from Kluchevskoy complex

	SiO_2	FeO	MnO	MgO	CaO	NiO	Total
Chromitite	40.98	5.47	0.10	52.64	0.03	0.46	99.68
Chromitite	41.12	4.63	0.08	52.88	n.d.	0.47	99.18
Chromitite	40.83	5.44	0.08	51.45	0.01	0.46	98.27
Dunite	40.97	9.13	0.13	48.14	0.03	0.20	98.60
Dunite	40.07	9.06	0.15	49.04	n.d.	0.17	98.49
Dunite	40.16	8.16	0.16	49.88	n.d.	0.30	98.66
Dunite	40.10	8.25	0.16	49.47	0.04	0.28	98.30
Dunite	41.02	7.85	0.11	51.54	n.d.	0.35	100.87
Dunite	40.96	7.58	0.13	50.06	n.d.	0.33	99.06
Dunite	41.59	7.75	0.55	48.59	n.d.	0.00	98.48
Harzburgite	39.51	9.44	0.13	49.74	n.d.	0.38	99.20
Wehrlite	40.50	8.77	0.16	49.82	n.d.	0.16	99.41
Wehrlite	40.09	9.08	0.11	49.93	n.d.	0.14	99.35
Wehrlite	40.55	8.85	0.11	49.90	n.d.	0.16	99.57
Wehrlite	39.28	12.40	0.27	47.24	n.d.	0.14	99.33

n.d. = not detected.

Table 1
Selected analyses (wt.%) of chromite from different rocks of the Kluchevkoy complex

	SiO_2	TiO_2	Al_2O_3	Cr_2O_3	FeO^{a}	MnO	MgO	NiO	ZnO	V_2O_3	Total
Chromitite	n.d.	0.16	11.74	58.76	17.63	0.25	12.91	0.05	0.21	0.09	101.80
Chromitite	0.09	0.14	10.11	57.74	17.18	0.31	12.37	0.29	0.13	0.07	98.42
Chromitite	0.09	0.14	11.36	58.54	18.11	0.29	13.57	0.07	0.15	0.17	102.48
Chromitite	0.12	0.14	10.90	57.78	17.68	0.30	11.55	0.25	n.d.	0.09	98.80
Chromitite	0.08	0.17	10.57	58.69	18.49	0.21	11.89	n.d.	0.17	0.07	100.33
Chromitite	0.04	0.22	12.13	53.26	23.77	0.43	9.55	0.18	0.11	n.d.	99.71
Chromitite	n.d.	0.21	12.50	54.89	21.51	0.30	11.75	0.02	0.03	0.31	101.62
Chromitite	0.05	0.20	12.01	53.75	21.75	0.39	11.34	0.17	n.d.	0.48	100.14
Chromitite	n.d.	0.19	11.66	53.87	23.44	0.52	9.16	0.18	0.30	0.33	99.66
Chromitite	n.d.	0.25	13.03	57.30	18.07	0.36	12.98	n.d.	n.d.	n.d.	101.99
Dunite	n.a.	0.18	9.66	59.09	21.39	0.50	9.14	0.16	0.15	n.a.	100.27
Dunite	n.a.	0.23	9.68	57.78	23.93	0.53	8.18	0.15	0.20	n.a.	100.68
Dunite	n.a.	0.23	9.21	56.91	26.20	0.54	6.80	0.13	0.19	n.a.	100.21
Dunite	n.a.	0.21	8.53	53.86	27.43	0.62	7.12	0.16	0.24	n.a.	98.17
Harzburgite	n.a.	0.05	19.34	49.02	20.80	0.41	10.42	0.12	0.18	n.a.	100.34
Wehrlite	n.a.	0.31	12.22	46.39	35.08	0.77	4.07	0.10	0.32	n.a.	99.26
Wehrlite	n.a.	0.28	12.71	46.11	35.37	0.87	4.29	0.16	0.63	n.a.	100.42
Wehrlite	n.a.	0.18	9.46	54.73	27.75	0.79	5.81	0.13	0.40	n.a.	99.25
Wehrlite	n.a.	0.15	8.43	55.26	25.75	0.72	6.57	0.12	0.24	n.a.	97.24

n.a. = not analyzed, n.d. = not detected.
[a] Total FeO.

Table 3
Representative analyses of PGM in the Kluchevskoy chromitites

Wt.%	Os	Ir	Ru	Rh	Pt	Pd	Ni	Fe	Cu	S	As	Tot
Laurite–erlichmanite												
KL8-6 1 2	19.77	8.24	35.34	1.08	n.d.	n.d.	0.04	n.d.	n.d.	32.46	n.d.	96.93
KL8-6 1 3	20.51	8.53	38.34	1.02	n.d.	n.d.	0.02	0.04	n.d.	32.37	n.d.	100.82
KL8-6 1 4	20.64	8.27	36.76	0.60	n.d.	0.08	0.14	0.05	n.d.	32.99	n.d.	99.53
KL8B II 3 2	12.21	7.66	41.75	0.78	n.d.	1.78	0.14	0.08	0.04	34.11	n.d.	98.54
KL8B II 3 5	12.48	7.71	41.67	0.62	n.d.	1.86	0.13	0.10	0.09	34.17	n.d.	98.83
KL9 2 5 2	15.50	10.8	37.51	0.86	n.d.	1.59	0.01	0.10	n.d.	33.27	n.d.	99.66
KL9 2 5 3	15.74	10.33	38.11	0.81	n.d.	1.71	0.07	n.d.	n.d.	34.63	n.d.	101.40
KL9 2 5 4	15.10	10.14	36.72	0.68	n.d.	1.60	0.10	0.17	0.08	32.77	n.d.	97.38
KL9 2 5 5	15.26	9.91	37.13	0.87	n.d.	1.57	0.11	0.11	n.d.	33.36	n.d.	98.32
KL8A I 2 2	58.36	11.65	2.69	0.09	n.d.	0.09	0.73	n.d.	n.d.	24.43	n.d.	98.04
PGE alloys												
KL8-6 2 2 A	24.44	25.03	48.75	1.36	0.48	n.d.	0.24	0.38	0.01	n.d.	n.d.	100.70
KL8B I 3 2	54.56	16.02	24.77	0.62	n.d.	0.29	2.30	n.d.	n.d.	n.d.	1.89	100.44
Ruthenarsenite												
KL8B I 3	7.63	1.25	40.89	1.43	0.59	0.55	6.02	0.31	n.d.	0.03	42.10	100.81
Ru-rich pentlandite												
KL8B I 2 2	5.66	3.34	7.00	0.51	n.d.	0.04	41.97	8.01	n.d.	30.53	2.71	99.77
KL9-1 11 4	0.22	0.46	10.34	1.00	n.d.	0.12	48.96	7.61	n.d.	32.42	n.d.	101.13
KL9-1 11 8	0.24	0.42	9.86	0.88	0.15	0.21	49.53	7.48	n.d.	32.69	0.20	101.66
Undefined (Ir,Os,Pt,Rh,Ni,Fe,Cu)$_6$S$_7$												
KL8A I 2 1	5.51	49.23	0.10	0.58	1.76	0.03	11.80	5.11	2.47	23.38	n.d.	99.96
Undefined (Ru,Os,Ir)$_5$(Ni,Fe,Cu)S$_8$												
KL9-1 11 2	20.65	7.75	36.05	0.21	n.d.	0.65	4.85	1.10	0.05	26.86	n.d.	98.18
Undefined (Ru,Os,Ni,Ir,Fe)S												
KL9-1 11 3	33.22	10.29	22.11	0.31	n.d.	0.27	10.41	1.95	n.d.	22.71	0.10	101.36
Undefined (Ru,Os,Ir)$_3$S$_2$												
KL9-1 11 6	43.37	8.85	30.34	0.16	n.d.	0.65	1.23	0.35	0.10	13.35	n.d.	98.40

At.%	Os	Ir	Ru	Rh	Pt	Pd	Ni	Fe	Cu	S	As
Laurite–erlichmanite											
KL8-6 1 2	6.84	2.82	23.00	0.69	n.d.	n.d.	0.04	n.d.	n.d.	66.61	n.d.
KL8-6 1 3	6.95	2.86	24.44	0.64	n.d.	n.d.	0.02	0.04	n.d.	65.05	n.d.
KL8-6 1 4	6.98	2.77	23.39	0.38	n.d.	0.05	0.15	0.06	n.d.	66.21	n.d.
KL8B II 3 2	3.99	2.48	25.66	0.47	n.d.	1.04	0.15	0.09	0.04	66.09	n.d.
KL8B II 3 5	4.07	2.49	25.56	0.37	n.d.	1.08	0.14	0.11	0.09	66.08	n.d.
KL9 2 5 2	5.19	3.58	23.61	0.53	n.d.	0.95	0.02	0.11	n.d.	66.02	n.d.
KL9 2 5 3	5.11	3.32	23.29	0.48	n.d.	0.99	0.07	n.d.	n.d.	66.73	n.d.
KL9 2 5 4	5.14	3.41	23.50	0.43	n.d.	0.98	0.11	0.20	0.09	66.14	n.d.
KL9 2 5 5	5.12	3.29	23.44	0.54	n.d.	0.94	0.12	0.13	n.d.	66.42	n.d.
KL8A I 2 2	26.22	5.18	2.28	0.07	n.d.	0.07	1.07	n.d.	n.d.	65.11	n.d.
PGE alloys											
KL8-6 2 2 A	16.74	16.96	62.80	1.73	0.32	n.d.	0.54	0.89	0.03	n.d.	n.d.
KL8B I 3 2	41.67	12.11	35.59	0.87	n.d.	0.40	5.69	n.d.	n.d.	n.d.	3.66
Ruthenarsenite											
KL8B I 3	3.51	0.57	35.35	1.21	0.27	0.46	8.96	0.49	n.d.	0.08	49.12

Table 3 (*continued*)

At.%	Os	Ir	Ru	Rh	Pt	Pd	Ni	Fe	Cu	S	As
Ru-rich pentlandite											
KL8B I 2 2	1.51	0.88	3.52	0.25	n.d.	0.02	36.32	7.29	n.d.	48.36	1.84
KL9-1 11 4	0.05	0.11	4.88	0.46	n.d.	0.05	39.75	6.50	n.d.	48.19	n.d.
KL9-1 11 8	0.06	0.10	4.62	0.41	0.04	0.09	39.94	6.34	n.d.	48.27	0.13
Unknown (Ir,Os,Pt,Rh,Ni,Fe,Cu)$_6$S$_7$											
KL8A I 2 1	2.13	18.81	0.07	0.41	0.66	0.02	14.76	6.72	2.85	53.56	n.d.
Unknown (Ru,Os,Ir)$_5$(Ni,Fe,Cu)S$_8$											
KL9-1 11 2	7.47	2.77	24.52	0.14	n.d.	0.42	5.69	1.36	0.05	57.59	n.d.
Unknown (Ru,Os,Ni,Ir,Fe)S											
KL9-1 11 3	12.71	3.90	15.91	0.22	n.d.	0.18	12.91	2.54	n.d.	51.54	0.09
Unknown (Ru,Os,Ir)$_3$S$_2$											
KL9-1 11 6	22.20	4.48	29.22	0.15	n.d.	0.60	2.03	0.62	0.15	40.55	n.d.

n.d. = not detected.

analyzed at the Universities of Modena and Reggio Emilia (Italy) and Granada (Spain).

4. Results

4.1. Composition of chromite, olivine and their thermometric significance

Despite the alteration that affected the Kluchevskoy complex, chromite is generally fresh, alteration being limited to development of ferrian–chromite along grains boundary and cracks. Therefore, the primary composition of chromite has been obtained in the preserved core of spinel grains. The content of the major oxides varies in the following ranges: Cr_2O_3 (63.08 to 49.89 wt.%), Al_2O_3 (14.93 to 9.13 wt.%), MgO (15.43 to 9.16 wt.%), FeO (19.06 to 9.38 wt.%), Fe_2O_3 (8.66 to 2.52 wt.%). The TiO_2 content is very low (<0.3 wt.%).

The investigated chromitites slightly differ form those associated with the mantle sequence of the ophiolite complexes of Kempirsai and Ray–Iz, being enriched in Fe^{2+} and showing higher TiO_2 contents and

lower $Cr/(Cr+Al)$ (Fig. 3). The analyses of massive chromite and disseminated cromite in dunite, harzburgite and wehrlite have been plotted in the TiO_2 *versus* Al_2O_3 diagram (Fig. 4). The composition of the Kluchevskoy chromites falls within the field of the supra-subduction zone (SSZ) peridotite as proposed by Kamenetsky et al. (2001).

Most of the investigated rocks exhibit partial to high degree of serpentinization, although relics of fresh olivine are frequent. Composition of olivine has been obtained on fresh crystals found associated with chromitite, dunite, harzburgite and wehrlite. We have applied the thermobarometer proposed by Ballhaus et al. (1991) to selected olivine–chromite pairs in the Kluchevskoy chromitite,

Table 4
Lithology and PGE concentrations of the analyzed samples

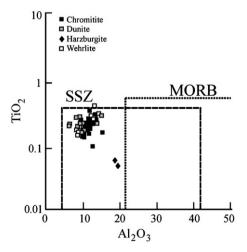|	Os	Ir	Ru	Rh	Pt	Pd	Au
Chromitite	8.3	19.5	45.1	6.2	2.0	1.3	1.1
Chromitite	6.5	15.3	42.3	7.1	2.7	1.3	1.4
Dunite	1.6	1.7	3.6	0.8	3.9	6.5	4.2
Dunite	1.5	1.3	4.5	1.1	3.5	2.7	2.8
Wehrlite	0.5	0.6	2.9	0.5	1.5	2.2	2.0
Wehrlite	0.5	0.9	2.4	1.3	12.2	10.6	2.8
Pyroxenite	0.6	0.6	2.5	0.7	27.9	26.8	3.6
Gabbro	0.2	0.1	1.9	0.2	2.7	1.3	2.3

Fig. 4. Composition of massive and disseminated chromite of the Kluchevskoy complex. Abbreviations: SSZ = supra-subduction zone, MORB = mid-ocean ridge basalts (Kamenetsky et al., 2001).

Table 5
Temperature ([Ballhaus et al., 1991](#)) for chromite–olivine pairs from Kluchevskoy chromitites

Data for Kempirai and Ray–Iz chromitite are reported for comparison

	Fe/ Fe+Mg	Mg/ Mg+Fe	Cr/ Cr+Al	$Fe^{3+}/$ $Fe^{2+}Fe^{3+}$	Fe	Mg	T °C
Kluchevskoy							
KL10-1	0.326	0.674	0.775	0.299	0.082	1.844	1040
KL10-2	0.326	0.674	0.775	0.299	0.045	1.916	823
KL10-3	0.326	0.674	0.775	0.299	0.052	1.870	876
KL10-4	0.326	0.674	0.775	0.299	0.048	1.844	852
KL10-5	0.326	0.674	0.775	0.299	0.046	1.887	835
KL8A-1	0.346	0.654	0.782	0.243	0.059	1.843	841
KL8A-2	0.346	0.654	0.782	0.243	0.052	1.858	802
KL8A-3	0.346	0.654	0.782	0.243	0.055	1.880	818
KL8A-4	0.346	0.654	0.782	0.243	0.054	1.845	817
KL8A-5	0.348	0.652	0.783	0.200	0.059	1.843	802
KL9-1	0.290	0.710	0.766	0.367	0.063	1.827	1072
KL9-2	0.290	0.710	0.766	0.367	0.056	1.918	1004
KL9-3	0.290	0.710	0.766	0.367	0.057	1.902	1016
KL9-4	0.290	0.710	0.766	0.367	0.057	1.832	1029
KL9-5	0.290	0.710	0.766	0.367	0.055	1.885	1003
Kempirsai							
KP-1	0.359	0.641	0.807	0.159	0.059	1.811	773
KP-2	0.372	0.628	0.804	0.135	0.088	1.803	851
KP-3	0.372	0.628	0.804	0.135	0.093	1.811	868
KP-4	0.372	0.628	0.804	0.135	0.095	1.787	879
KP-5	0.359	0.641	0.807	0.159	0.088	1.803	896
KP-6	0.359	0.641	0.807	0.159	0.093	1.811	914
Ray–Iz							
RZ-1	0.316	0.684	0.782	0.189	0.057	1.934	807
RZ-2	0.332	0.668	0.793	0.132	0.048	1.921	701
RZ-3	0.314	0.686	0.788	0.214	0.054	1.845	840
RZ-4	0.329	0.671	0.795	0.185	0.056	1.891	800
RZ-5	0.298	0.702	0.782	0.283	0.064	1.890	970
RZ-6	0.387	0.613	0.846	0.182	0.063	1.904	781

and in the Kempirsai and Ray–Iz for comparison. The obtained temperatures in the chromitite of Kluchevskoy vary in the range 802 to 1072 °C, whereas those obtained in the Kempirsai and Ray–Iz chromitites fall between 701 and 970 °C ([Table 5](#)).

4.2. Distribution of PGE and Au

Total PGE concentrations in the analyzed chromitites are very low and range from 75 to 82 ppb; the Au content is 1 ppb ([Table 4](#)). Chondrite-normalized distribution patterns of the Kluchevskoy chromitites are presented in [Fig. 5](#)A, and compared with those of the chromitites from mantle hosted ophiolites of Kempirsai and Ray–Iz and the Al-rich chromitites of Kempirsai ([Melcher et al., 1999;](#) [Kojonen et al., 2003](#) and unpublished data of the authors). The Kluchevskoy chromitites are similar to the Al-rich chromitites of Kempirsai, as far as Os–Ir–Ru concentra-

tions are concerned, whereas the patterns of Rh–Pt–Pd–Au are more consistent with those of the mantle hosted ophiolite chromitites ([Fig. 5](#)). The $(Os+Ir+Ru)/(Rh+Pt+Pd)$ ratio in the Kluchevskoy chromitites varies from 5.8 to 7.7, suggesting an enrichment in $Os+Ir+Ru$ over $Rh+Pt+Pd$, as typical of a number of mantle ophiolite-hosted chromitites.

The PGE concentrations in dunite, wehrlite, pyroxenite and gabbro of the Kluchevskoy complex, normalized to chondrite, have been plotted in [Fig. 5](#)B. The analyzed dunites and one wehrlite display some similarities with those of the Kempirsai ophiolite, although they are characterized by lower concentrations of Os, Ir and Ru. Gabbro, pyroxenite and one wehrlite of the Kluchevskoy complex show positive PGE patterns, although this positive trend is less pronounced in the gabbro because of a strong Ru positive anomaly respect to Rh ([Fig. 5](#)B). In contrast to the chromitites, the dunite, wehrlite, pyroxenite and gabbro do not display enrichment of $(Os+Ir+Ru)$ over $(Rh+Pt+Pd)$ and the ratio between these two groups of elements falls between 0.1 and 1.0. Nevertheless, all the analyzed rocks of the Kluchevskoy complex display enrichment in Ru ([Fig. 5](#)).

4.3. PGE mineralogy

The PGM found in the Kluchevskoy chromitites consists of Ru–Os–Ir minerals; phases of Rh–Pt–Pd are absent. Therefore, the results of the mineralogical study are fully consistent with the geochemical data. The PGM are generally less than 10 μm in size and in most cases, form composite grain of two or more PGM and base metal sulfides. The PGM population displays large mineralogical variability with the following PGM identified: laurite, erlichmanite, cuproiridsite, irarsite, ruthenarsenite, osmium, iridium, ruthenium, Ru-rich pentlandite and a series of unnamed PGE-base metals (BM) sulfides. The mineral assemblage of the Kluchevskoy chromitites resembles most mantle ophiolite-hosted chromitites worldwide ([Stockman and Hlava, 1984;](#) [Augé and Johan, 1988;](#) [McElduff and Stumpfl, 1990;](#) [Nilsson, 1990;](#) [Thalhammer et al., 1990;](#) [Garuti and Zaccarini, 1997;](#) [Garuti et al., 1999c;](#) [Uysal et al., 2005;](#) [Zaccarini et al., 2005](#)) and also from the Urals ([Anikina et al., 1996;](#) [Melcher et al., 1997;](#) [Garuti et al., 1999a](#)), and is characterized by abundant Os–Ir–Ru minerals and the absence of Rh–Pt–Pd phases. Based on both textural and paragenetic evidence, the PGM of the Kluchevskoy chromitites can be divided into two distinct groups:

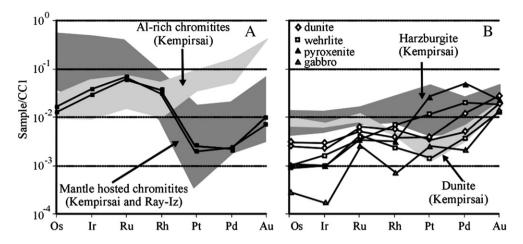1) Primary PGM, formed in the high-temperature magmatic stage before, during, and after the

Fig. 5. C1 chondrite (Naldrett and Duke, 1980) normalized patterns. A = The Kluchevskoy chromitites (black square) compared with the chromitites hosted in the ophiolites of Kempirsai and Ray–Iz (data from Melcher et al., 1999; Kojonen et al., 2003 and unpublished data of the authors). B = Mafic–ultramafic rocks of Kluchevskoy complex in comparison with dunite and harzburgite of Kempirsai (data source: unpublished data of the authors).

precipitation of chromite. They are found completely included in fresh chromite crystals and display a polygonal shape.

2) Secondary PGM, altered at low temperature, during some post-magmatic event. The secondary PGM occur in contact with altered minerals, mainly chlorite and ferrian–chromite and characterized by an irregular shape.

Examples of the morphology and textural relations of the PGM are illustrated in Fig. 6, and selected microprobe analyses are reported in Table 3.

The most common PGM found in the investigated chromitites is laurite, as is typical for the ophiolite chromitites. It occurs as single phase crystal or forms composite grains with other PGM, BM sulfides and silicates (mainly pargasite, clinopyroxene and chlorite, Fig. 6C–F). All the single phase laurite crystals are polygonal and included in fresh chromite. Laurite grains, that occur associated with chlorite, other PGM and Ru-rich pentlandite, are characterized by a sub-euhedral shape (Fig. 6D,F).

Erlichmanite is very rare and only one grain was analyzed, occurring included in fresh chromite and associated with iridium, and undefined PGE-BM sulfide corresponding to the formula $(Ir_{2.45}Os_{0.28}Pt_{0.09}Rh_{0.05}Ni_{1.92}Fe_{0.87}Cu_{0.37})_{6.04}S_{6.96}$ (Fig. 6B). This PGM is brownish in color and shows a distinct anisotropy similar to pyrrhotite, although the Ni > Fe composition is not consistent with this conclusion.

The composition of the Kluchevskoy laurite–erlichmanite series has been plotted, as atomic %, in a Ru–Os–Ir ternary diagram (Fig. 7) and compared with the

compositions of laurite–erlichmanite associated with the mantle hosted chromitites from Ray–Iz and Kempirsai ophiolites. Laurite–erlichmanite phases are similar in composition, although the Kluchevskoy laurite displays lower contents of Ir. In both, the Kluchevskoy and Ray–Iz chromitites laurite is more abundant than erlichmanite. On the contrary, at Kempirsai erlichmanite is the dominant PGM (Fig. 7).

Ruthenarsenite was found in association with Os–Ir alloys, included in fresh chromite (Fig. 6A). Repeated microprobe analyses can be recalculated to give the average formula $(Ru_{0.69}Os_{0.06}Rh_{0.03}Ir_{0.01}Ni_{0.16}Fe_{0.03})_{0.98}As_{1.02}$.

Irarsite and cuproiridsite were only qualitatively identified. Irarsite occurs with laurite in one composite grain located within a fissure (Fig. 6E). Cuproiridsite has been observed frequently attached to the edges of the laurite crystals (Fig. 6C).

Iridium and one Os–Ir alloy were found included in fresh chromite as polygonal crystals in polyphase grains associated with erlichmanite and unnamed $(Ir_{2.45}Os_{0.28}Pt_{0.09}Rh_{0.05}Ni_{1.92}Fe_{0.87}Cu_{0.37})_{6.04}S_{6.96}$ and ruthenarsenite, respectively (Fig. 6A,B). Owing its small size, iridium was only qualitatively analyzed. The Os–Ir alloy, according to the nomenclature proposed by Harris and Cabri (1991) was classified as osmium. Its composition, plotted in the Ru–Os–Ir ternary diagram and compared with magmatic PGE alloys from the Ray–Iz and Kempirsai chromitites, is characterized by high Ru and low Ir contents (Fig. 8). Other Ru–Os alloys, classified as ruthenium (Fig. 8), display an anhedral morphology and they are observed to replace laurite along the grain boundaries, typically associated
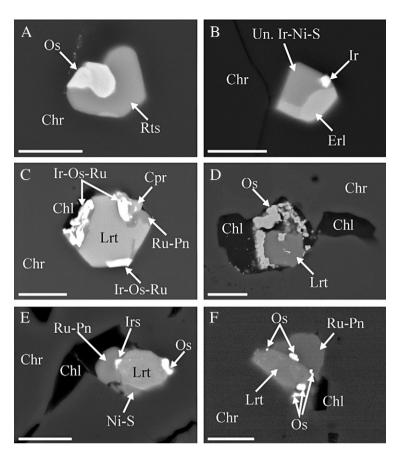
Fig. 6. Scanning electron microscope images showing morphology, texture and mineral assemblage of the Kluchevskoy PGM. Abbreviations: Os = osmium, Rts = ruthenarsenite, Chr = chromite, Un. Ir–Ni–S = unknown Ir–Ni sulfide, Ir = iridium, Erl = erlichmanite, Ir–Os–Ru = Ir–Os–Ru alloy, Lrt = laurite, Cpr = cuproiridsite, Ru–Pn = Ru-rich pentlandite, Chl = chlorite, Irs = irarsite, Ni–S = Ni sulfide. Scale bar = 5 μm.

with chlorite and ferrian chromite (Fig. 6D). Their compositions, in terms of Ru–Os–Ir concentrations, overlap the laurite field, suggesting a possible genetic relation by desulfurization of the sulfides at low temperature, as reported by Stockman and Hlava (1984) and Garuti and Zaccarini (1997).

5. Discussion and conclusions

5.1. Chromite and olivine

The large chromite deposits of Kempirsai, Voikar–Syninski and Ray–Iz in the Urals occur, unequivocally, in the mantle sequence of a supra-subduction zone ophiolite. According to the genetic model proposed by Melcher et al. (1997, 1999), the large chromite ore deposits of Kempirsai formed or re-crystallized as consequence of a metasomatic reaction between fluids and a depleted mantle. Based on mineralogical, petrological and structural analogies, Garuti et al. (1999a) proposed that a similar fluid-induced metasomatism was active also in the

residual mantle of the Polar Urals, and was possibly responsible for the formation and re-equilibration of the chromite deposits at Ray–Iz. The temperatures for the
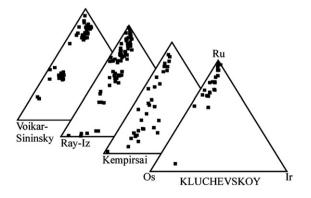

Fig. 7. Composition (atomic %) of laurite–erlichmanite series from different ophiolitic chromitites from the Urals. Data source: Kluchevskoy, present work; Kempirsai, Melcher et al. (1997) and unpublished data of the authors; Ray–Iz, Garuti et al. (1999a); Voikar–Sininsky, Anikina et al. (1996).
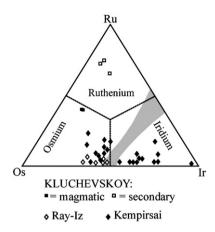
Fig. 8. Composition of the analyzed alloys from the Kluchevskoy chromitites, given as atomic %. Composition of alloys from Ray–Iz and Kempirsai chromitites are reported for comparison (data from Melcher et al., 1997 and Garuti et al., 1999a). The nomenclature and miscibility gap (gray field) are those of Harris and Cabri (1991).

chromitites of Kempirsai and Ray–Iz, based on Fe–Mg partitioning between olivine and spinel, are below 1000 °C in a range comprises between 701 and 970 °C. These temperatures are probably consistent with the proposed metasomatic reaction that occurred in both complexes. The thermal range registered in the Kluchevskoy chromitite expands up to 1070 °C, suggesting that the Kluchevskoy chromitite suffered the effects of the metasomatism to a lesser extent. The composition of chromite has been used as a good petrogenetic indicator, since many years, especially to discriminate stratiform and podiform chromitites. Recently it has been shown that it is also possible to distinguish chromite formed in supra-subduction from those originated in mid-ocean ridge basalts on the basis of Al_2O_3 and TiO_2 contents (Kamenetsky et al., 2001). The composition of massive and disseminated chromite in dunite, harzburgite and wehrlite of the Kluchevskoy complex is consistent with a supra-subduction zone geodynamic setting (Kamenetsky et al., 2001). Furthermore, the Kluchevskoy chromitites are characterized by high Cr_2O_3 and low TiO_2 contents, typical of the chromitites crystallized from a boninitic melt (Arai, 1992).

5.2. PGE and PGM

High-Cr chromitites forming from melt-rock inter-action or magma mixing involving liquidus of boninitic composition are extremely enriched in Ru–Os–Ir over Rh–Pt–Pd. This may be explained by early extraction of Ru–Os–Ir with chromite from the melt, with the more incompatible Rh–Pt–Pd remaining in the melt (Melcher et al., 1999).

The PGE distribution in the Kluchevskoy chromitites indicates that they are enriched in Ru–Os–Ir compared to Rh–Pt–Pd as typical for the high-Cr chromitites. The predominance of Ru–Os–Ir minerals, and the absence of Rh–Pt–Pd specific phases in the Kluchevskoy chromi-tite, is fully consistent with these geochemical data.

It has been demonstrated that the crystallization and paragenesis of magmatic PGM from major chromitite deposits in ophiolite is strongly influenced by the sulfur fugacity and temperature (Nakagawa and Franco, 1997; Melcher et al., 1997, 1999; Garuti et al., 1999a,c). In particular, at high temperature and low sulfur fugacity, Ru-rich laurite coexists with Os–Ir–Ru alloys. The presence of abundant erlichmanite accompanied by other Os–Ir–Ru sulfides is indicative of relatively low temperature and/or high sulfur fugacity.

Detailed study of textural relations shows that the majority of the PGM in the Kluchevskoy chromitite were mechanically trapped in growing chromite crystals at high temperature. The magmatic paragenesis is characterized by the presence of abundant Ru-bearing minerals and the scarcity of Os and Ir specific minerals that, on the contrary, are frequent in the Kempirsai, Ray–Iz and Voikar–Sininsky mantle hosted chromi-tites. Furthermore, laurite from Kluchevskoy has a lower Ir content than those reported from Kempirsai, Ray–Iz and Voikar–Sininsky laurite (Anikina et al., 1996; Melcher et al., 1997; Garuti et al., 1999a).

This mineralogical observation suggests that the precipitation of PGM in the Kempirsai and Ray–Iz chromitite occurred at low temperature and high sulfur fugacity, whereas in the Kluchevskoy chromitite the PGM crystallized at lower sulfur fugacity and/or higher temperature. This mineralogical observation is, thus, fully consistent with the temperature calculated from the olivine–spinel geothermometer.

Some PGM in the Kluchevskoy chromitite have been altered and reworked after their crystallization. In particular, replacement of laurite grains by Ru–Os–Ir alloys is interpreted as the result of incipient desulfur-ization process occurred at low temperature and possibly during the serpentinization as reported in the literature (Stockman and Hlava, 1984; Garuti and Zaccarini, 1997; Garuti et al., 1997b, 1999a; Zaccarini et al., 2005).

References

Anikina, Y.V., Moloshag, V.P., Alimov, V.Y., Kononkova, N.N., 1996. Type chemistry of laurite from Polar Ural alpine-type hyperbasite. Doklady Russian Academy of Sciences. Earth Sciences Sections 345, 410–412.

Arai, S., 1992. Chemistry of chromian spinel in volcanic rocks as a potential guide to magma chemistry. Mineralogical Magazine 56, 173–784.

Augé, T., Johan, Z., 1988. Comparative study of chromite deposits from Troodos, Vourinos, North Oman and New Caledonia ophiolites. In: Boissonnas, J., Omenetto, P. (Eds.), Mineral Deposits Within the European Community. Springer-Verlag, Berlin, Germany, pp. 267–288.

Ballhaus, C., Berry, R.F., Green, D.H., 1991. High pressure experimental calibration on the olivine–orthopyroxene–spinel oxygen geobarometer: implications for the oxidation state of the upper mantle. Contributions to Mineralogy and Petrology 107, 27–40.

Distler, V.V., Kryachko, V.V., Yudovskaya, M.A., 2003. Formation of platinum-group metals in chromite ores of the Kempirsai ore field. Geology of Ore Deposits 45, 37–65.

Donovan, J.J., Rivers, M.L., 1990. PRSUPR—a PC based automation and analyses software package for wavelength dispersive electron beam microanalyses. Microbeam Analysis 66–68.

Economou-Eliopoulos, M., Zhelyaskova-Panayotova, M., 1998. Comparative study of the geochemistry of chromite ores from the Kempirsai (Urals) and Rhodope (Balkan Peninsula) ophiolite massifs. Bulletin, Geological Society of Greece 32, 203–211.

Ferrario, A., Garuti, G., 1988. Platinum group minerals in chromite-rich horizons of the Niquelandia complex (Central Goias, Brazil). In: Prichard, H.M., Potts, P.J., Bowles, J.F.W., Cribb, S.J. (Eds.), Geo-platinum, vol. 87. Elsevier Applied Sciences, London, pp. 261–272.

Fershtater, G.B., Bea, F., Borodina, N.S., Montero, M.P., Smirnov, V.N., Pushkarev, E.V., Rappaport, M.S., Zinger, T.F., 1997. Magmatism as a key to deep Urals. In: Perez-Estuan, A., Brown, D., Gee, D. (Eds.), EUROPROBE'S Uralides Project. Tectonophysics, vol. 276, pp. 87–102.

Garuti, G., Zaccarini, F., 1997. In situ alteration of platinum-group minerals at low temperature: evidence from serpentinized and weathered chromitite of the Vourinos complex, Greece. The Canadian Mineralogist 35, 611–626.

Garuti, G., Fershtater, G.B., Bea, F., Montero, P., Pushkarev, E.V., Zaccarini, F., 1997a. Platinum-group elements as petrological indicators in mafic–ultramafic complexes of central and southern Urals: preliminary results. Tectonophysics 276, 181–194.

Garuti, G., Zaccarini, F., Cabella, R., Fershtater, G.B., 1997b. Occurrence of unknown Ru–Os–Ir–Fe oxides in the chromitites of the Nurali ultramafic complex, southern Urals, Russia. The Canadian Mineralogist 35, 1431–1439.

Garuti, G., Zaccarini, F., Moloshag, V., Alimov, V., 1999a. Platinum-group minerals as indicator of sulfur fugacity in ophiolitic upper mantle: an example from chromitites of the Ray–Iz ultramafic complex (Polar Urals, Russia). The Canadian Mineralogist 37, 1099–1115.

Garuti, G., Zaccarini, F., Cabella, R., Pushkarev, E., Smirnov, V., 1999b. Occurrence of platinum-group minerals in chromitites of the Kluchevskoy ophiolite complex, Central Urals, Russia: preliminary results. In: Stanley, C.J., et al. (Ed.), Mineral Deposits: Processes to Processing. Balkema, Rotterdam, pp. 721–723.

Garuti, G., Zaccarini, F., Economou-Eliopoulos, M., 1999c. Paragenesis and composition of laurite in chromitites of Othrys (Greece): implication for Os–Ru fractionation in ophiolitic upper mantle of the Balkan Peninsula. Mineralium Deposita 34, 312–319.

Harris, D.C., Cabri, J.L., 1991. Nomenclature of platinum group elements alloys: review and revision. The Canadian Mineralogist 29, 231–237.

Kamenetsky, V.S., Crawford, A.J., Meffre, S., 2001. Factors controlling chemistry of magmatic spinel: an empirical study of associated olivine, Cr-spinel and melt inclusions from primitive rocks. Journal of Petrology 42, 655–671.

Kojonen, K., Zaccarini, F., Garuti, G., 2003. Platinum-Group elements and gold geochemistry and mineralogy in the Ray–Iz ophiolitic chromitites, Polar Urals. In: Eliopoulos, D.G., et al. (Ed.), Mineral Exploration and Sustainable Development. Millpress, Rotterdam, pp. 599–602.

Kravchenko, G.G., 1986. Geological position and structure of chromite deposits in the Ural mountains. In: Petrascheck, W., Karamata, S., Kravchenko, G.G., Johan, Z., Economou, M., Engin, T. (Eds.), Chromites, Theophrastus Publications S.A., Athens, pp. 3–21.

McElduff, B., Stumpfl, E.F., 1990. The chromite deposits of the Troodos complex, Cyprus — evidence for the role of a fluid phase accompanying chromite formation. Mineralium Deposita 26, 307–318.

Melcher, F., Grum, W., Simon, G., Thalhammer, T.V., Stumpfl, E.F., 1997. Petrogenesis of the ophiolitic giant chromite deposits of Kempirsai, Kazakhstan: a study of solid and fluid inclusions in chromite. Journal of Petrology 38, 1419–1458.

Melcher, F., Grum, W., Thalhammer, T.V., Thalhammer, O.A.R., 1999. The giant chromite deposits at Kempirsai, Urals: constraints from trace elements (PGE, REE) and isotope data. Mineralium Deposita 34, 250–272.

Nakagawa, M., Franco, H.E.A., 1997. Placer Os–Ir–Ru alloys and sulfides: indicators of sulfur fagacity in an ophiolite? The Canadian Mineralogist 35, 1441–1452.

Naldrett, A.J., Duke, J.M., 1980. Pt metals in magmatic sulfide ores. Science 208, 1417–1424.

Nilsson, L.P., 1990. Platinum-group mineral inclusions in chromitite from Osthammeren ultramafic tectonite body, south central Norway. Mineralogy and Petrology 42, 249–263.

Stockman, H.W., Hlava, P.F., 1984. Platinum-group minerals in Alpine chromitites from south-western Oregon. Economic Geology 79, 491–508.

Thalhammer, O.A.R., Prochaska, W., Mühlans, H.W., 1990. Solid inclusion in chrome-spinels and platinum-group element concentration from the Hochgrössen and Kraubath ultramafic massifs (Austria). Contributions to Mineralogy and Petrology 105, 66–80.

Uysal, I., Sadiklar, M.B., Tarkian, M., Karsli, O., Aydin, F., 2005. Mineralogy and composition of the chromitites and their platinum-group minerals from Ortaga (Mugla-SW Turkey): evidence for ophiolitic chromitite genesis. Mineralogy and Petrology 83, 219–242.

Zaccarini, F., Pushkarev, E.V., Fershtater, G.B., Garuti, G., 2004. Composition and mineralogy of PGE-rich chromitites in the Nurali lehrzolite–gabbro complex. Southern Urals, Russia. The Canadian Mineralogist 42, 545–562.

Zaccarini, F., Proenza, J.A., Ortega-Gutiérrez, F., Garuti, G., 2005. Platinum-group minerals in ophiolitic chromitites from Tehuitzingo (Acatlán complex, southern Mexico): implications for post-magmatic modification. Mineralogy and Petrology 84, 147–168.